OFFICE OF NAVAL RESEARCH

Contract N00014-91-J-1475

Technical Report No. 3

A ROBUST ALGORITHM FOR ISOTROPIC RECONSTRUCTION OF MAGIC-ANGLE SPINNING SOLID-STATE NMR SPECTRA

by

N. C. Elbaum and J. F. Haw

Submitted to

Analytical Chemistry

Department of Chemistry
Texas A&M University
College Station, TX 77843

SECURITY CLASSIFICATION OF THIS PAGE

REPORT DOCUMENTATION PAGE

1a. REPORT SECURITY CLASSIFICATION none	1b. RESTRICTIVE MARKINGS none
2a. SECURITY CLASSIFICATION AUTHORITY none	3. DISTRIBUTION / AVAILABILITY OF REPORT unlimited
2b. DECLASSIFICATION / DOWNGRADING SCHEDULE none	
4. PERFORMING ORGANIZATION REPORT NUMBER(S) Technical Report #3	5. MONITORING ORGANIZATION REPORT NUMBER(S)
6a. NAME OF PERFORMING ORGANIZATION Texas A&M University 6b. OFFICE SYMBOL (If applicable)	7a. NAME OF MONITORING ORGANIZATION Office of Naval Research
6c. ADDRESS (City, State, and ZIP Code) Dept. of Chemistry, MS # 3255 Texas A&M University College Station, TX 77843-3255	7b. ADDRESS (City, State, and ZIP Code) Chemistry Division 800 North Quincy Street Arlington, VA 22217-5000
8a. NAME OF FUNDING / SPONSORING ORGANIZATION Office of Naval Research 8b. OFFICE SYMBOL (If applicable)	9. PROCUREMENT INSTRUMENT IDENTIFICATION NUMBER
8c. ADDRESS (City, State, and ZIP Code) Chemistry Division 800 North Quincy Street Arlington, VA 22217-5000	10. SOURCE OF FUNDING NUMBERS PROGRAM ELEMENT NO. / PROJECT NO. / TASK NO. / WORK UNIT ACCESSION NO

11. TITLE (Include Security Classification)

A Robust Algorithm for Isotropic Reconstruction of Magic-Angle Spinning Solid-State NMR Spectr

12. PERSONAL AUTHOR(S)
Nick C. Elbaum and James F. Haw

13a. TYPE OF REPORT	13b. TIME COVERED	14 DATE OF REPORT (Year, Month, Day)	15. PAGE COUNT
Technical	FROM 1/1/92 TO 4/22/92	4/23/92	

16. SUPPLEMENTARY NOTATION

Submitted to Analytical Chemistry

17. COSATI CODES			18. SUBJECT TERMS (Continue on reverse if necessary and identify by block number)
FIELD	GROUP	SUB-GROUP	

19. ABSTRACT

Magic-angle spinning (MAS) is an essential component of most solid state NMR experiments. The use of finite spinning speeds results in spinning sidebands due to incomplete averaging of chemical shift anisotropy or quadrupole effects. Sidebands can seriously affect interpretation and quantitation, and the need to minimize them has had a pervasive influence on the practice of MAS NMR. We report a radically new approach for reconstructing spectra in the limit of infinite spinning speed from a set of experimental spectra obtained at various finite speeds. This is achieved using a robust algorithm that handles any number of sideband orders and deals with overlapping peaks. The full signal-to-noise advantage of acquiring multiple spectra is preserved in the reconstruction.

Isotropic reconstruction is illustrated for ^{13}C CP/MAS spectra for crystalline compounds and a representative polymer, ^{13}P MAS spectra of a mixture, and ^{79}Br MAS spectra of KBr. 19 orders of sidebands were used in the reconstruction of the latter example.

A limitation of the present algorithm is that it requires spectra to be obtained at speeds sufficient to resolve the sidebands from the isotropic peaks. It thus fails to reconstruct the ^{13}C CP/MAS spectrum of a coal from experimental spectra at very slow spinning speeds.

20. DISTRIBUTION / AVAILABILITY OF ABSTRACT	21 ABSTRACT SECURITY CLASSIFICATION
☑ UNCLASSIFIED/UNLIMITED ☑ SAME AS RPT ☐ DTIC USERS	
22a NAME OF RESPONSIBLE INDIVIDUAL Dr. James F. Haw	22b TELEPHONE (Include Area Code) 409/845-1966
	22c OFFICE SYMBOL

DD FORM 1473, 84 MAR 83 APR edition may be used until exhausted
All other editions are obsolete

SECURITY CLASSIFICATION OF THIS PAGE

A Robust Algorithm for Isotropic Reconstruction of Magic-Angle Spinning Solid-State NMR Spectra

Nick C. Elbaum and James F. Haw*

Department of Chemistry, Texas A&M University, College Station, Texas 77843

Abstract

Magic-angle spinning (MAS) is an essential component of most solid state NMR experiments. The use of finite spinning speeds results in spinning sidebands due to incomplete averaging of chemical shift anisotropy or quadrupole effects. Sidebands can seriously affect interpretation and quantitation, and the need to minimize them has had a pervasive influence on the practice of MAS NMR. We report a radically new approach for reconstructing spectra in the limit of infinite spinning speed from a set of experimental spectra obtained at various finite speeds. This is achieved using a robust algorithm that handles any number of sideband orders and deals with overlapping peaks. The full signal-to-noise advantage of acquiring multiple spectra is preserved in the reconstruction.

Isotropic reconstruction is illustrated for ^{13}C CP/MAS spectra for crystalline compounds and a representative polymer, ^{13}P MAS spectra of a mixture, and ^{79}Br MAS spectra of KBr. 19 orders of sidebands were used in the reconstruction of the latter example.

A limitation of the present algorithm is that it requires spectra to be obtained at speeds sufficient to resolve the sidebands from the isotropic peaks. It thus fails to reconstruct the ^{13}C CP/MAS spectrum of a coal from experimental spectra at very slow spinning speeds.

*Author to whom correspondence should be addressed

Upcoming Research

A major problem is solid state NMR has been addressed using a radically new approach. The advantages of infinite spinning speed are obtained from spectra at slow speeds by calculation.

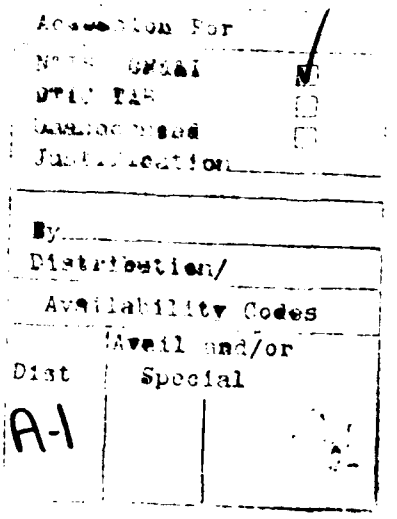

Introduction

High resolution solid state NMR experiments are used to characterize the properties of polymers, catalysts, fossil fuels, and other important materials and compounds(*1-3*). Currently, nearly all high resolution solid state spectra of spin-1/2 nuclei are obtained using a technique called magic-angle spinning (MAS) to average the orientation dependence of the chemical shift interaction, achieving line narrowing. Detailed descriptions of the theory of NMR of rotating solids have been published elsewhere (*4,5*). Briefly, if the sample spinning rate is greater than the width (in frequency units) of the chemical shift anisotropy interaction, a single relatively sharp resonance is obtained at the isotropic chemical shift for every inequivalent site. At sufficiently high rotation rates, therefore, MAS NMR spectra of solid compounds are reminiscent of analogous spectra of solutions.

If the spinning speed is not appreciably greater than the widths of the chemical shift anisotropies, the resulting spectra are more complicated. For the case of rare spins (i.e., neglecting a homogeneous dipolar coupling) slow speed MAS spectra are characterized by signals at the isotropic chemical shifts accompanied by rotational sidebands separated from the isotropic frequencies by $\pm n\omega$ where ω is the spinning speed and n is an integer. This behavior is depicted in the ^{13}C MAS spectra simulated for a 7.05-T magnetic field (75.36 MHz) shown in Figure 1. As suggested by those simulations, the sideband patterns generated by finite spinning speeds can cause problems in interpretation. The spectrum simulated at a spinning speed of 2000 Hz is crowded by peaks, although all but two are sidebands. For sufficiently complicated spectra, it may not even be possible to classify the isotropic peaks and associated sidebands without obtaining spectra at two or more spinning speeds. Furthermore, since the total peak intensity is partitioned into the isotropic peak and the spinning sidebands, quantitation of spectral intensities is difficult in many cases. The spectrum simulated at a spinning speed of 3500 Hz presents a particularly difficult problem of interpretation and quantitation, because there is mutual centerband/sideband overlap and sideband/sideband overlap.

The obvious solution to the above problem is to spin at sufficiently high rates that the sideband intensities are negligible. The upper limit for ^{13}C chemical shift anisotropy in typical organic compounds is ca. 120 ppm (*6*). For a typical magnetic field strength of 7.05 T (corresponding to a ^{1}H resonance frequency of 300 MHz) this implies a minimum spinning speed of at least 9.0 kHz. On an 11.9-T system (i.e., 500-MHz ^{1}H frequency) the minimum requirement would be at least 15 kHz. These spinning speeds are achievable with current technology (*7*), but not without several penalties. High speed designs generally require rotors with small outer diameters and often thicker walls in order to achieve high rotation rates and maintain those rates without catastrophic failure. For a given spinning system design, doubling the spinning speed requires reducing the sample payload by a factor of two to four. Furthermore, high speed spinning systems are also much more prone to wear and catastrophic failure and are generally less reliable than systems designed for slower speeds. One cannot, therefore, spin at higher speeds without trade-offs, and most of the MAS spectra reported in the literature in recent years have been obtained at spinning rates of 3-6 kHz. Although such rates are usually adequate for experiments at lower field strengths, ^{13}C MAS spectra of rigid solids obtained at 7.05 T or higher typically show two or more orders of spinning sidebands for the aromatic and carbonyl resonances.

Since NMR signal strength is directly proportional to sample payload and proportional to the magnetic field to ca. the three-half's power, signal-to-noise considerations alone would suggest that most experiments should be done with a large sample at the highest available field strength. Hence, slow speed experiments are attractive when high sensitivity and/or short measurement times are important (*8,9*). Furthermore, high speed magic-angle spinning has a deleterious effect on the dynamics of cross polarization which is very commonly used to generate the NMR signal for ^{13}C, ^{15}N and other rare spins (*10*). Schemes have been proposed to minimize this problem (*11*) but it is probable that CP/MAS spectra obtained at spinning speeds greater than 6 kHz should be considered

only semiquantitative until proven otherwise.

Thus, the requirement to rotate the sample fast enough to reduce the sideband intensities to an acceptable level handicaps some experiments and has a pervasive influence on the practice of solid state NMR including probe research and development and magnetic field preference.

Several different approaches have been suggested for acquiring sideband-free spectra at low spinning speeds. Usually these methods eliminate the sidebands without correcting for the intensity lost from the isotropic peaks. One class of experiments, originally developed by Dixon (*12*) and elaborated upon on by Griffin and coworkers (*13*) uses a series of pulses during the rotational period to alternate the phases of the sidebands, allowing for their cancellation. These sequences discriminate against signals with short T_2 values and can also fail when the chemical shift anisotropy is very large or if there are timing errors or electronic instabilities.

Other strategies for reducing sideband intensities that have been proposed from time to time include modulation of the spinning speed (smearing out the sidebands) or taking the square root of the product of two spectra at different speeds. The above methods do not yield the correct isotropic peak intensities. Simple mathematical methods such as the last cited can fail spectacularly in various pathological, but common situations. For example, if the spectra in Figure 1 simulated at 3000 and 4000 Hz were multiplied together, isotropic peaks would be falsely recognized at 91 and 109 ppm.

Our strategy has been to recognize that all of the information necessary to reconstruct the spectrum at hypothetical infinite spinning speed is usually present in a set of MAS spectra acquired at several different, but slow, spinning speeds. We term this approach isotropic reconstruction. Recently, we communicated the use of a primitive isotropic reconstruction formula that gave acceptable results provided that only one order of sidebands was present and several other restrictive conditions were met (*14*). The present report describes the development of a robust algorithm that allows isotropic reconstruction to be performed for much more general cases. We demonstrate that

this algorithm works on peaks which exhibit as many as 19 orders of spinning sidebands and on a variety of sample types that are representative of the most commonly encountered in MAS NMR studies. For nearly all of the samples studied, the isotropic reconstruction algorithm eliminates all sidebands, recovers the correct intensities of the isotropic peaks, and preserves all of the signal-to-noise inherent in the acquisition of multiple spectra. The exception to successful reconstruction are spectra with very broad features such as the case of ^{13}C MAS spectra of coal, for which the present algorithm fails due to the relative lack of baseline between the features of those spectra.

Experimental Section

Reagents. Disperse red I (2-{N-ethyl-p-[(p-nitrophenyl)azo]anilino}ethanol), hexamethylbenzene, glycine and KBr were obtained from Aldrich. Pyrophosphate and Trimetaphosphate were obtained from Sigma. The polyethylene terephthalate sample was provided by W. R. Grace.

NMR Spectroscopy. All spectra were acquired on a Chemagnetics CMX-300 spectrometer at a field strength of 7.05 T. Magic-angle spinning spectra were acquired using 7.5-mm (o.d.) zirconia pencil rotors with Kel-F drive tips and caps. Spinning speeds were controlled to an accuracy of ca. 1 Hz using a Chemagnetics spin speed controller.

The method of excitation (i.e CP vs. 90° flip) used was the one best suited for each sample. Enough data points were used in each spectrum such that the digital resolution was several times smaller than the narrowest spectral feature. Typically 10-12 spectra were obtained per sample over a range of spinning speeds from 2.0 to 5.5 kHz.

Data Format. Free induction decays were transferred to a 486-based computer over an Ethernet connection. All spectra in a given data set were transformed and phased (using common values of the phase parameters) using the software package Felix® (Hare Associates). The set of transformed spectra, ordered in increasing spinning speed, was then used as the input data matrix for

the isotropic reconstruction algorithm. Our isotropic reconstruction program assumes an ASCII format, but transliteration routines for other data formats exist, or are easily written.

Isotropic Reconstruction Program. The algorithm was encoded in the Microsoft QuickBasic® language and run on the 486 computer. A typical data set of 10-12 spectra, each consisting of 1-K points, required about 3 seconds of computation time for isotropic reconstruction. Original spectra as well as intermediate and final results are displayed on a VGA monitor and/or plotted on a laser-jet printer accepting HPGL output. A copy of the program is available from the author upon written request.

Results and Discussion

The isotropic reconstruction algorithm is most easily explained by a worked example. First we will introduce a result and show that the algorithm eliminates sidebands, recovers correct isotropic intensities, and provides the full signal-to-noise advantage of acquiring multiple spectra. Then using that example, we will explain how the algorithm processes the set of spectra to classify isotropic peaks and sidebands and reconstructs the spectrum in the limit of infinite spinning speed. After analyzing that example in detail, we illustrate the broad applicability of the present algorithm to more complicated sideband problems. Finally we show a weakness of the present algorithm that applies when the peaks are so broad that resolution of isotropic peaks and their associated sidebands is not achieved at any of the spinning speeds used.

Figure 2 shows ^{13}C CP/MAS spectra of a mixture of hexamethylbenzene (HMB) and glycine. This sample generates four isotropic peaks: the glycine carboxyl at 177 ppm; the HMB aromatic at 132 ppm; the glycine methylene at 46 ppm; and the HMB methyl at 17 ppm. The 177- and 132-ppm resonances have significant chemical shift anisotropies resulting in one or two orders of sidebands at 7.05 T and moderate spinning speeds. Ten spectra were acquired with spinning speeds ranging from 2750 to 5000 Hz, and representative spectra are shown in Figure 2. Overlap of first-order sidebands

and isotropic peaks is seen in the spectrum at 3500 Hz.

The uppermost spectrum in Figure 2 shows the calculated spectrum obtained by isotropic reconstruction of the full ten-spectrum data set using the new algorithm. This spectrum is completely free of sidebands and shows no obvious artifacts. The intensities in this spectrum are accurate to better than 3 %. (A small difference in integrated intensities of the 177-ppm peak vs. the 17-ppm peak is due to a slight Hartmann-Hahn mismatch and is also reflected in all of the experimental spectra.) The expanded plots of the baselines show that the algorithm preserved the signal-to-noise inherent in the coaddition of the ten spectra.

A flow chart of the major steps in the algorithm is shown in Figure 3. Most of the steps are concerned with the classification of peaks as either isotropic or sideband of various order and source. Figure 4 shows all ten of the spectra used in the isotropic reconstruction depicted in Figure 2. The vertical and diagonal lines in Figure 4 designate the maxima of peaks classified by the algorithm as isotropic or sideband, respectively. The algorithm actually treats each frequency (point) above the noise threshold as a peak, but for clarity only the points at peak maxima are labeled in the figure. Thus, line shape information is preserved by treating each resonance as ten or more discrete "peaks" depending on the digital resolution and line width. Inspecting Figure 4, one notes that the algorithm has successfully identified all four isotropic peaks, all four first-order sidebands, and those second-order sidebands that are above the noise threshold in three or more spectra.

The isotropic reconstruction program starts by reading in the individual transformed spectra into a matrix arranged in increasing spinning order. This matrix is indexed along each row by spinning speed, ω, and each column by frequency, f. The spectral intensity at a particular point in the matrix is designated by $I(f,\omega)$. The matrix depicted in Figure 4 is of dimension 1024 by 10. The program then does a preliminary analysis of the data to calculate a noise threshold and scale the intensities to a minimum value of 1 and a maximum value of 1000. This scaling prevents error

conditions and minimizes loss of precision in subsequent computations.

A column analysis of the matrix identifies isotropic peaks by examining all of the intensities in each column (for each f, consider all ω). A flowchart of this step is shown in Figure 5. If intensity above the noise threshold is found in every spectrum at the current value of f, that frequency is designated as isotropic. The identification of sidebands and the recognition of overlap conditions is carried out in the next two steps of the algorithm. A row analysis then examines each spectrum separately as shown in the flowchart in Figure 6. For every isotropic peak identified in the column analysis, the intensities are examined at $f \pm n\omega$, where n is the order of the sideband. If intensity above the noise threshold is found, that element of the matrix is marked as potentially a sideband associated with the isotropic peak at frequency f. If the frequency $f \pm n\omega$ was previously identified as also being an isotropic peak, then the element of the matrix being considered is also labeled as potentially a case of sideband-isotropic overlap. Final classification of sidebands and identification of overlap conditions is achieved by diagonal analyses of the data matrix, as shown by the flowchart in Figure 7. For every frequency designated as a potential sideband in a given row, ω, sidebands of the same order are searched for in the other rows. If these are found in more than three rows (without overlap), the diagonal is classified as a sideband of order n from the isotropic peak at frequency f, I_f.

Sideband-isotropic and/or sideband-sideband overlap conditions are set for each matrix element which is has more than one classification. Consider again the experimental data matrix in Figure 4 which shows several examples of sideband-isotropic overlap. The spectrum obtained at 3250 Hz is characterized by overlap of the isotropic peak at 177 ppm with the negative first-order sideband from the 132-ppm resonance, overlap of the isotropic peak at 132 ppm with the positive first-order sideband from the 177-ppm peak, and overlap of the positive second-order sideband of 132 ppm with the isotropic peak at 46 ppm.

Having classified the isotropic peaks and sidebands and identified some of the matrix elements as having intensities due to two or more components (overlap conditions), the algorithm then reconstructs each individual row (spectrum) in the matrix. This process is outlined in the flowchart in Figure 8. If overlap were not possible, reconstruction would simply be a matter of adding sideband intensities at $f \pm n\omega, \omega$ back into the appropriate isotropic peaks at f, ω. Elements in the matrix that have been identified as overlap situations must have their intensity values decomposed into the two or more components responsible for the overlap. This is done through statistical fits of columns of intensity data for isotropic peaks and fits of diagonal intensity data for sidebands. Figure 9 is a plot of peak intensity vs. spinning speed for the isotropic peak at 177 ppm in the experimental data matrix in Figure 4, i.e., it is a plot of $I(f,\omega)$ for the column f at the maximum of the peak. The matrix element at ω = 3250 Hz was previously classified as a case of sideband-isotropic overlap (see Figure 4), and the intensity of that spinning speed clearly departs from the smooth curve suggested by the other data points in Figure 9. The algorithm fits the nine valid (non-overlapped) points in Figure 9 to a suitable equation (vide infra), and then recalculates the intensity of the isotropic peak at any given spinning speed from that equation. Note that although the data point at 3250 Hz is not used because of overlap in the example shown, the intensity of the isotropic peak at 3250 Hz is predicted from the statistical fit, without a contribution from overlap. Analogous fitting procedures are used to isolate sideband intensities in cases of sideband-isotropic and sideband-sideband overlap. In some cases, intensity values are corrected by removing an overlap contribution before being used as a now-valid intensity in the next fitting step. Several hundred such statistical fits are used in a typical isotropic reconstruction of a data matrix with 1-K columns.

Once the intensities of all isotropic and sideband peaks have been recalculated and tabulated for each row (spectrum) in the matrix, each spectrum is individually reconstructed by adding the sideband intensities to the appropriate isotropic intensities. This is suggested by the following

equation

$$IR\ (f,\omega) = I'(f,\omega) + \Sigma\ I'(f+n\omega,\omega)$$

where IR (f,ω) is the reconstructed intensity at a given frequency, and the primed intensities are the recalculated values (ideally) free of overlap contributions. Signal averaging is obtained in the final step by summing the intensities in each column to give a single spectrum.

The nature of the equation used to fit I vs. ω data such as those in Figure 9 deserves comment. Theoretical treatments of the intensities of sidebands as a function of spinning speed and the principal components of the individual chemical shift tensor have been published (*4,5*). At first glance, fitting curves like Figure 9 to a theoretically sound form seems like a compelling goal, and indeed it might be necessary to do so if reconstruction were to be done by literally extrapolating intensity data to the limit of infinite spinning speed. But the present algorithm, unlike its primitive predecessor (*14*), does not rely on extrapolation outside of the range of experimental spinning speeds. Rather, it makes use of interpolations, as necessary, to resolve overlap conditions. It is not necessary to fit data like Figure 9 to a theoretically justifiable form, it is only necessary to select a function that fits the data well. Furthermore, the formalism for accurately describing sideband intensities often involves lengthy calculations and may not apply in cases of partially oriented materials or overlapping isotropic peaks. The data in Figure 9 suggest that a simple exponential dependence of intensity on spinning speed would provide a reasonable fit, and this has proven to be a useful assumption. For example, the valid data in Figure 9 were fit to an equation of the form

$$I(f,\omega) = a_f - b_f e^{-k_f \omega}$$

where a_f, b_f, and k_f are constants used in the fitting of column f. Analogous equations are used to fit sideband intensities to exponential functions of spinning speed. In practice, we linearize these equations and fit the natural log of intensity to spinning speed to take advantage of the decreased

computation time and increased accuracy of linear least-squares fits relative to nonlinear fitting routines.

Having explained in detail how the new algorithm works, we now show several examples which illustrate the usefulness of isotropic reconstruction to MAS NMR spectra of representative samples. Figure 10 shows that the algorithm successfully reconstructs the ^{13}C CP/MAS spectrum of the azo dye disperse red I ($C_{16}H_{18}N_4O_3$) from spectra obtained at 12 spinning speeds, three of which are shown. The algorithm's ability to preserve line shape information is suggested by the reconstruction of the ^{13}C CP/MAS spectrum of poly(ethylene terephthalate) shown in Figure 11. The inset in the reconstructed spectrum clearly shows the shoulder on the low-shielding side of the methylene signal which has previously been assigned to the amorphous fraction of the polymer (*15*). This inset also emphasizes the 29.3 Hz/point digital resolution in the reconstruction due to the use of 1-K data sets. Digital resolution could be improved by using larger data sets with a modest increase in computation time, or alternatively, by inverse Fourier transform of the reconstructed spectrum, zero filling, and then transforming back to the frequency domain.

Atoms with more electrons than carbon can have more anisotropic nuclear shielding as well. The ^{31}P MAS spectra of a mixture of sodium pyrophosphate and sodium metaphosphate in Figure 12 show at least five orders of sidebands, and the isotropic peaks are not even recognizable in the spectra obtained at lower spinning speeds. This data set was also reconstructed correctly by the new algorithm. Spinning sidebands in MAS spectra arise not only from chemical shift anisotropy, but in the case of the central transition of non-integer quadrupolar spins, the second-order quadrupole effect as well. The most familiar example is the ^{79}Br spectrum of KBr (*16*), as illustrated in Figure 13. In this case, the algorithm classified sidebands as high as nineteenth order and reconstructed all other intensity into the isotropic peak. In all of the examples shown above, the accuracy of the intensities in the reconstructed spectra were typically accurate within 2-5 % as determined by

comparison of integrated intensity in the reconstructed spectrum to the total integrated intensity above the noise threshold in the original data matrix.

We are aware of only one common situation in which the present isotropic reconstruction algorithm fails. When the spectral features are broader than the higher spinning speeds used, the sidebands will not be separated from their own first order sidebands at any point in the data matrix, and several errors will result. Some columns will contain sideband intensities at all speeds and will be falsely recognized as isotropic peaks. Furthermore, it may not be possible to fit intensity vs. spinning speed data when many overlap conditions reduce the degrees of freedom below the number of parameters which must be fit. Figure 14 shows the failure of the current algorithm for the ^{13}C CP/MAS spectrum of a bituminous coal sample. The reconstructed spectrum is to a first approximation just the sum of the slow speed spectra in the data set because of the classification problems discussed above. A less-severe failure was also obtained when we tried to reconstruct the ^{13}C CP/MAS spectrum of lignin, which is also relatively broad.

In conclusion, the new isotropic reconstruction algorithm is clearly more robust than its primitive predecessor. Spectra with multiple orders of sidebands and extensive overlap at some speeds are reconstructed with few or no artifacts and retention of the signal-to-noise advantage inherent in the acquisition of multiple spectra. Line shape information is preserved, and the present algorithm may be suited for the study of synthetic polymers without further improvement. It also appears to be useful for simplifying MAS spectra of quadrupolar nuclei, and this application deserves further attention. The current algorithm fails when the peaks are so broad that the sidebands are not fully resolved at even the higher spinning speeds used. Although this problem could always be dealt with by spinning at somewhat higher speeds or using somewhat lower fields than those used in the present investigation (e.g., 2.5 - 5 kHz and 7.05 T), this obvious solution seems contrary to the spirit that lead us to undertake the development of isotropic reconstruction. Our suspicion is that it will be possible

to develop improved methods for reconstructing sets of broad MAS spectra such as that from which the slow speed spectra in Figure 14 were taken.

Acknowledgement

This work was supported by the Office of Naval Research (Grant# N00014-88-K-0239) and the National Science Foundation (Grant CHE-8918741). We would like to thank Robert Wind and Dean Sindorf of Chemagnetics for their suggestions and encouragement.

References

(1) Yannoni, C. S. *Acc. Chem. Res.* **1982**, *15*, 201.

(2) Fyfe, C. A. *Solid State NMR for Chemists*; C.F.C. Press: Ontario, 1983.

(3) Maciel, G. E. *Science* **1984**, *226*, 282.

(4) Maricq, M. M.; Waugh, J. S. *J. Chem. Phys.* **1979**, *70*, 3300.

(5) Herzfeld, J.; Berger, A. E. *J. Chem. Phys.* **1980**, *73*, 6021.

(6) Duncan, T. M. *A Compilation of Chemical Shift Anisotropies*; Farragut Press: Madison, 1990.

(7) Dec, S. F.; Wind, R. A.; Maciel, G. E.; Anthonio, F. E. *J. Magn. Reson.* **1986**, *70*, 355.

(8) Zhang, M.; Maciel, G. E. *Anal. Chem.* **1990**, *63*, 633.

(9) Zhang, M.; Maciel, G. E. *J. Magn. Reson.* **1989**, *85*, 156.

(10) Sardashti, M.; Maciel, G. E. *J. Magn. Reson.* **1987**, *72*, 467.

(11) Barbara, T. M.; Brooks, A. B.; Williams, E. H. Presented at the Experimental NMR Conference, St. Louis, Missouri, April 1991; poster 153.

(12) Dixon, W. T.; Schaefer, J.; Sefick, M. D.; Stejskal, E. O.; McKay, R. A. *J. Magn. Reson.* **1982**, *49*, 341.

(13) Raleigh, D. P.; Olejniczak, E. T.; Vega, S.; Griffin, R. G. *J. Magn. Reson.* **1987**, *72*, 238.

(14) Elbaum, N. C.; Haw, J. F. *J. Magn. Reson.* **1991**, *91*, 199.

(15) Sefcik, M. D.; Schaefer, J.; Stejskal, E. O.; McKay, R. A. *Macromolecules* **1980**, *13*, 1132.

(16) Frye, J. S.; Maciel, G. E. *J. Magn. Reson.* **1982**, *48*, 125.

Figure Captions

Figure 1. Simulated 75.36-MHz ^{13}C MAS spectra illustrating the effects of finite spinning speeds. The parameters for the isotropic peak at 70 ppm are σ_{11}=20 ppm, σ_{22}=70 ppm, and σ_{33}=120 ppm. those parameters for the isotropic peak at 160 ppm are σ_{11}=100 ppm, σ_{22}=160 ppm, and σ_{33}=220 ppm.

Figure 2. Demonstration of the isotropic reconstruction procedure for a mixture of hexamethylbenzene and glycine. Three of the ten experimental ^{13}C CP/MAS spectra are shown along with the reconstructed spectrum.

Figure 3. Flowchart showing the major steps of the isotropic reconstruction algorithm.

Figure 4. The full ten-spectra data matrix used in the reconstruction of the HMB-glycine mixture (see text).

Figure 5. Flowchart of the column analysis which recognizes isotropic peaks.

Figure 6. The row analysis of the algorithm finds the sidebands associated with isotropic peaks by following the steps in this flowchart.

Figure 7. Flowchart of the diagonal analysis used to confirm sidebands.

Figure 8. Flowchart of the reconstruction steps of the algorithm.

Figure 9. A representative column slice taken at 46 ppm from the data matrix in Figure 4. These data show the variation in peak intensity with spinning speed (see text).

Figure 10. Isotropic reconstruction of the ^{13}C CP/MAS spectra of disperse red 1. Three of twelve experimental spectra are shown.

Figure 11. Isotropic reconstruction of the ^{13}C CP/MAS spectrum of poly(ethylene terephthalate). Three of ten experimental spectra are shown. The inset is an enhanced view of the peak at ca. 60 ppm showing the preservation of line shape by the reconstruction algorithm.

Figure 12. Isotropic reconstruction of the ^{31}P MAS spectrum of a mixture of pyrophosphate and trimetaphosphate. Three of twelve experimental spectra are also shown.

Figure 13. Application of isotropic reconstruction to a quadrupolar nucleus, ^{79}Br of KBr. The many orders of sidebands are emphasized in the expanded plots.

Figure 14. The limitation of the present algorithm is illustrated for the ^{13}C CP/MAS spectrum of a Bituminous coal (see text).

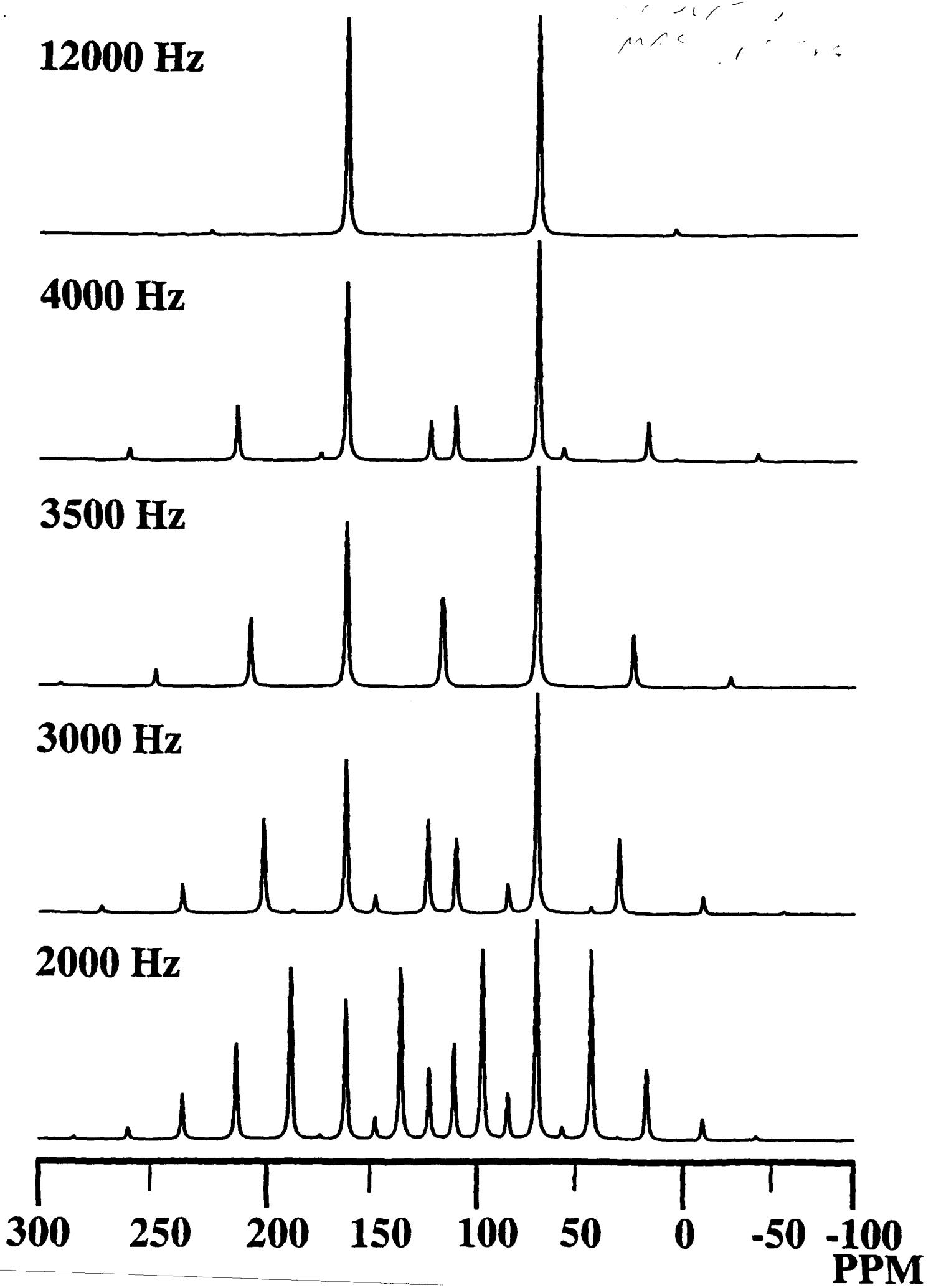
12000 Hz
4000 Hz
3500 Hz
3000 Hz
2000 Hz
300
250
200
150
100
50
0
-50
-100
PPM

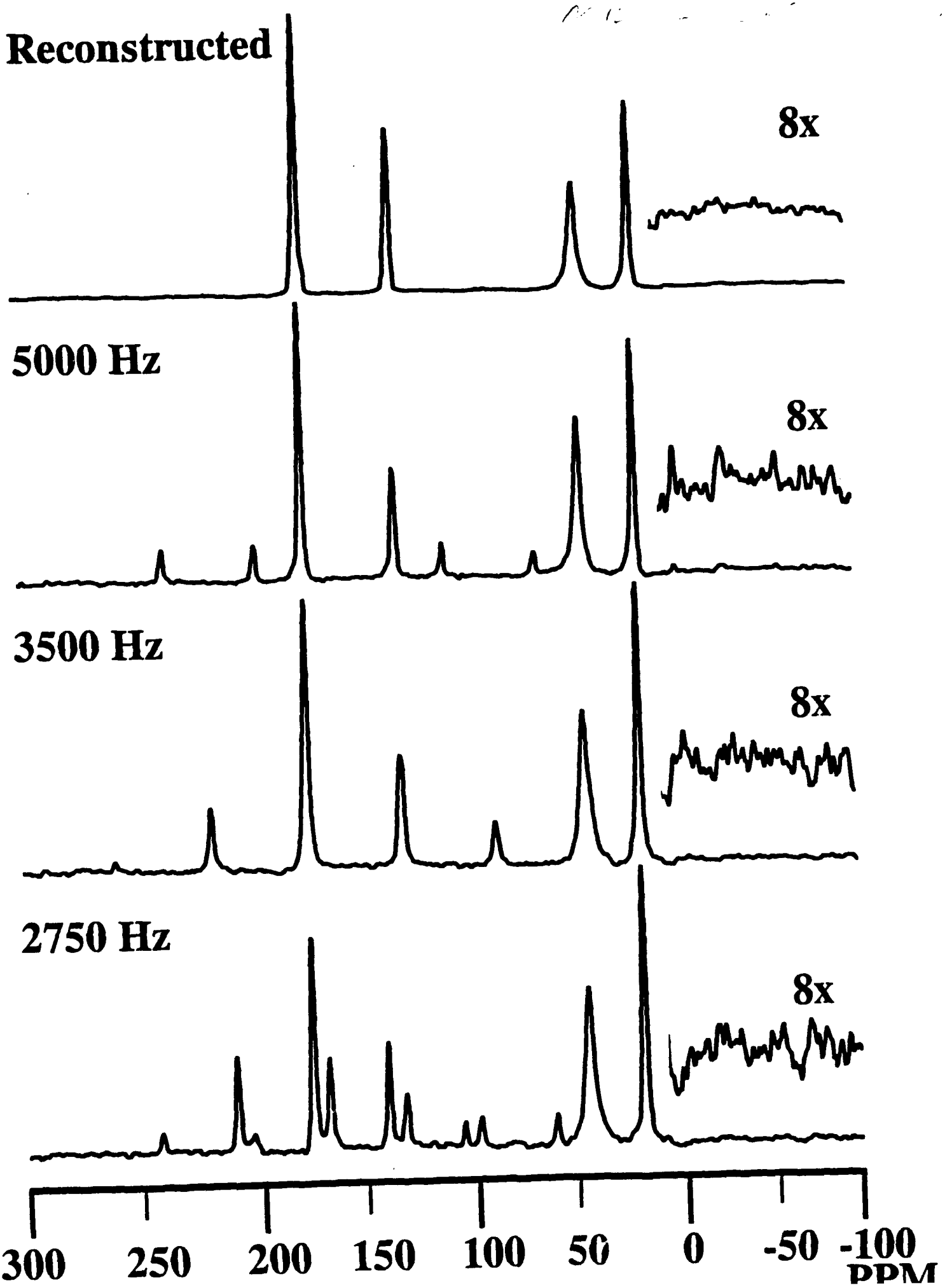
Reconstructed
8x
5000 Hz
8x
3500 Hz
8x
2750 Hz
8x
300
250
200
150
100
50
0
-50
-100
PPM

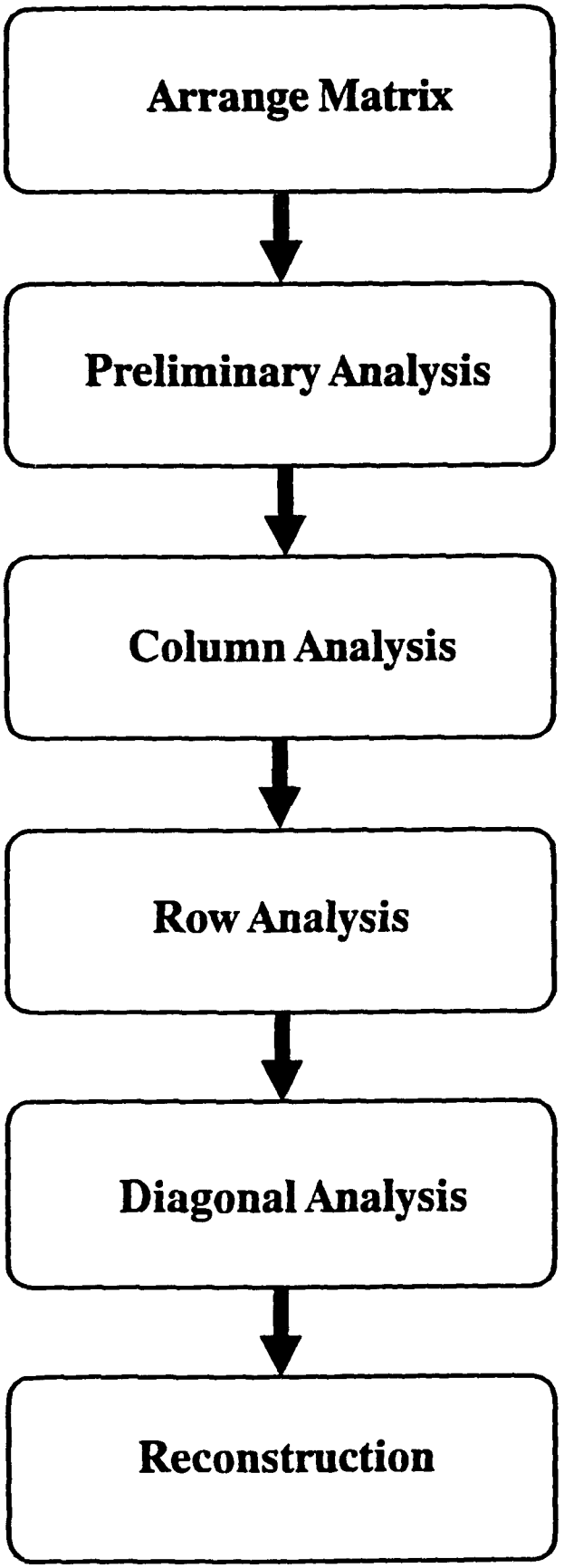
Arrange Matrix
Preliminary Analysis
Column Analysis
Row Analysis
Diagonal Analysis
Reconstruction

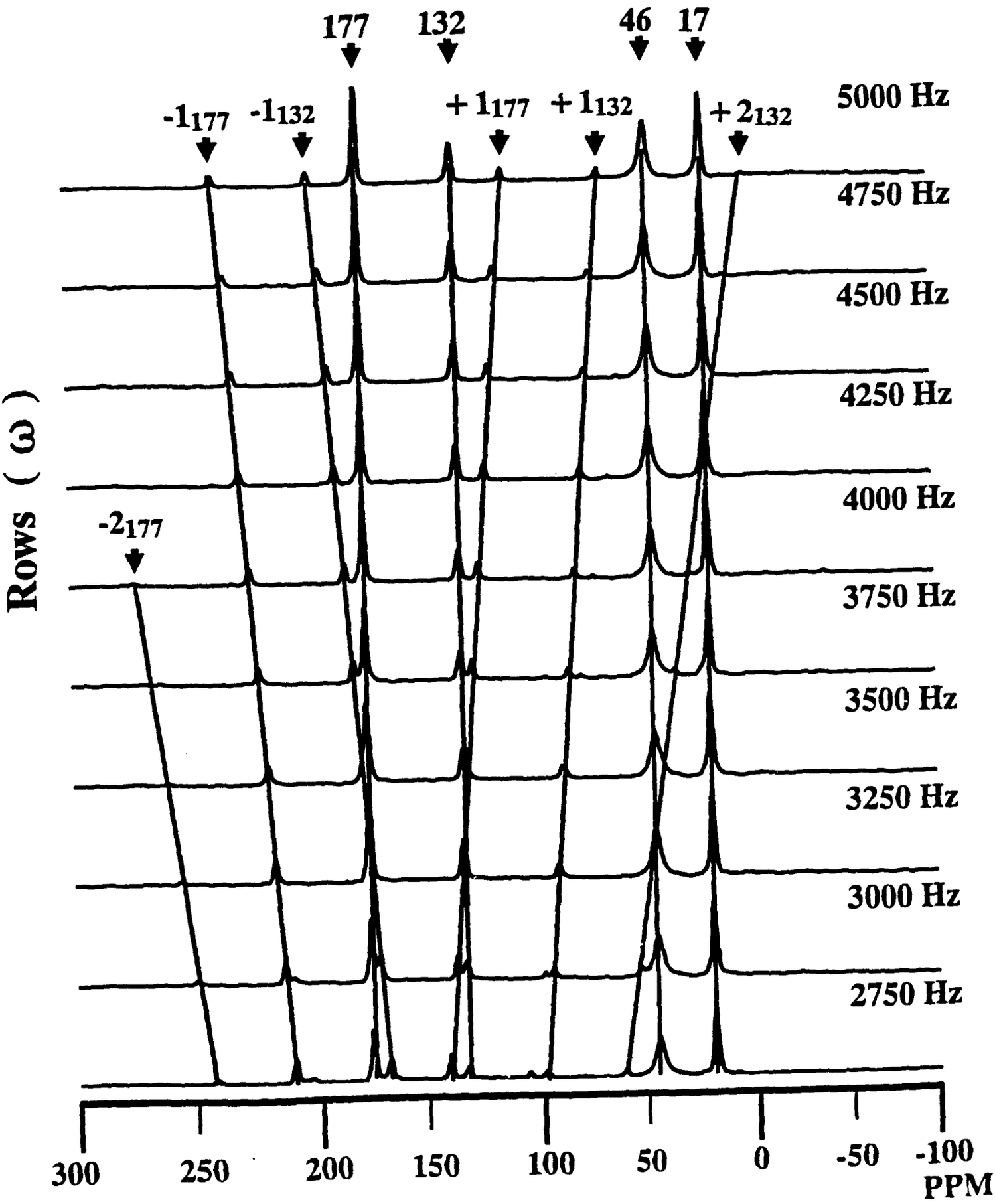
Columns (f)
177
132
46
17
-1177
-1132
+1177
+1132
+2132
5000 Hz
4750 Hz
4500 Hz
4250 Hz
4000 Hz
-2177
3750 Hz
3500 Hz
3250 Hz
3000 Hz
2750 Hz
Rows (ω)
300
250
200
150
100
50
0
-50
-100
PPM

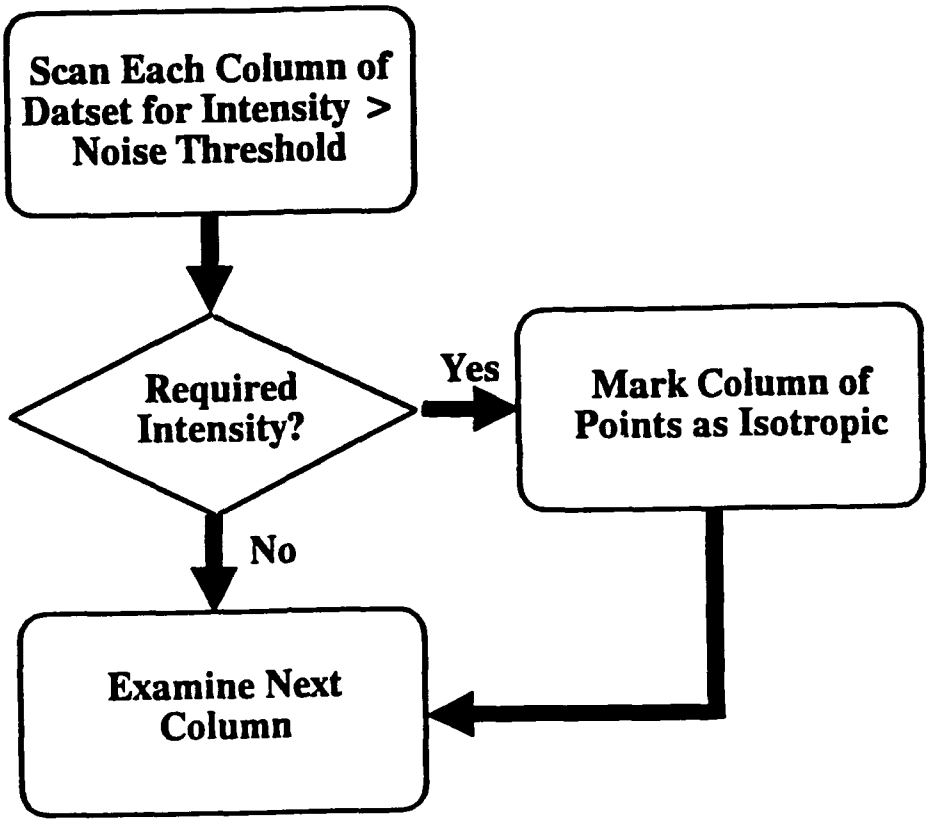
Scan Each Column of Datset for Intensity > Noise Threshold
Required Intensity?
Yes
Mark Column of Points as Isotropic
No
Examine Next Column

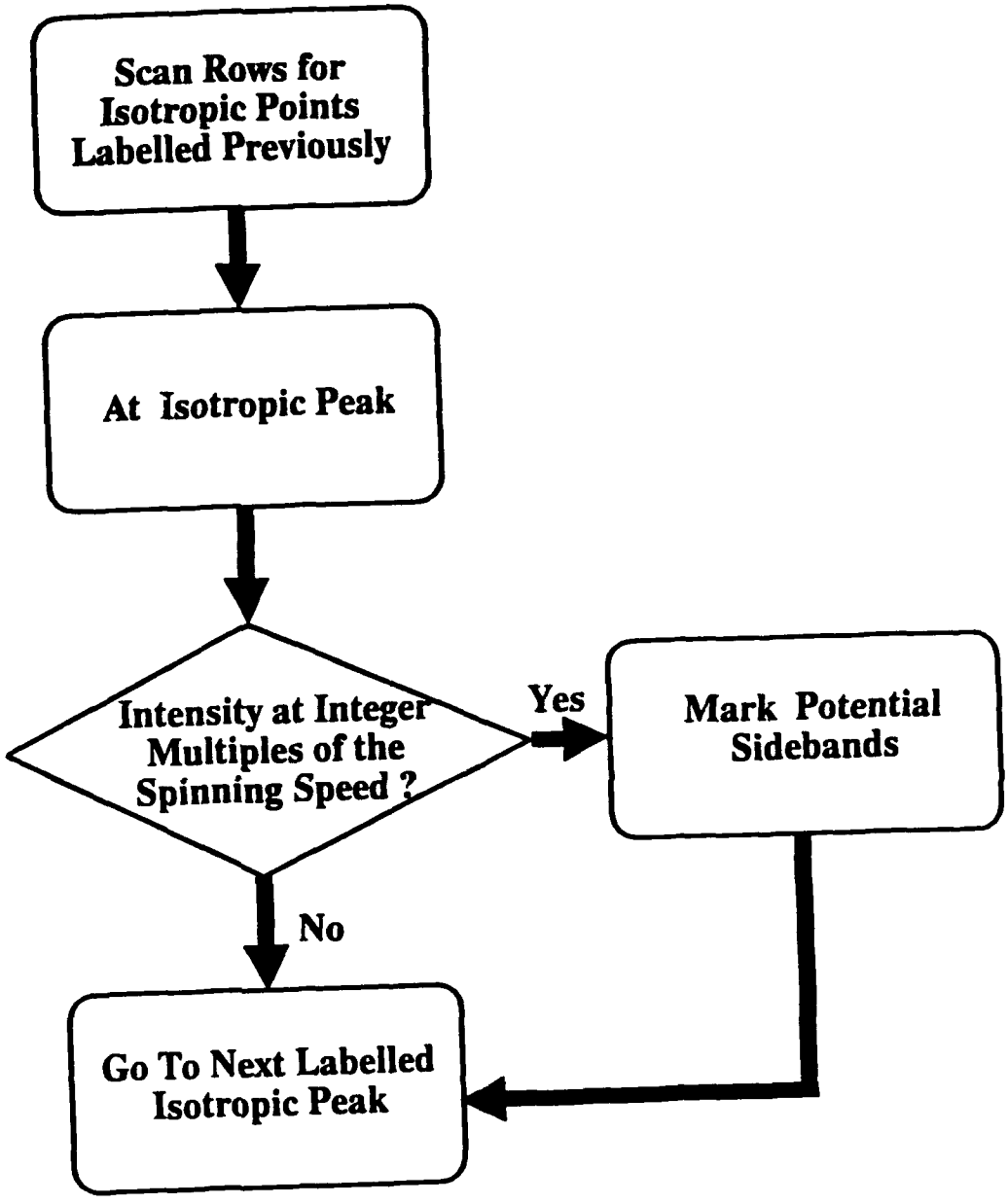
Scan Rows for Isotropic Points Labelled Previously
At Isotropic Peak
Intensity at Integer Multiples of the Spinning Speed ?
Yes
Mark Potential Sidebands
No
Go To Next Labelled Isotropic Peak

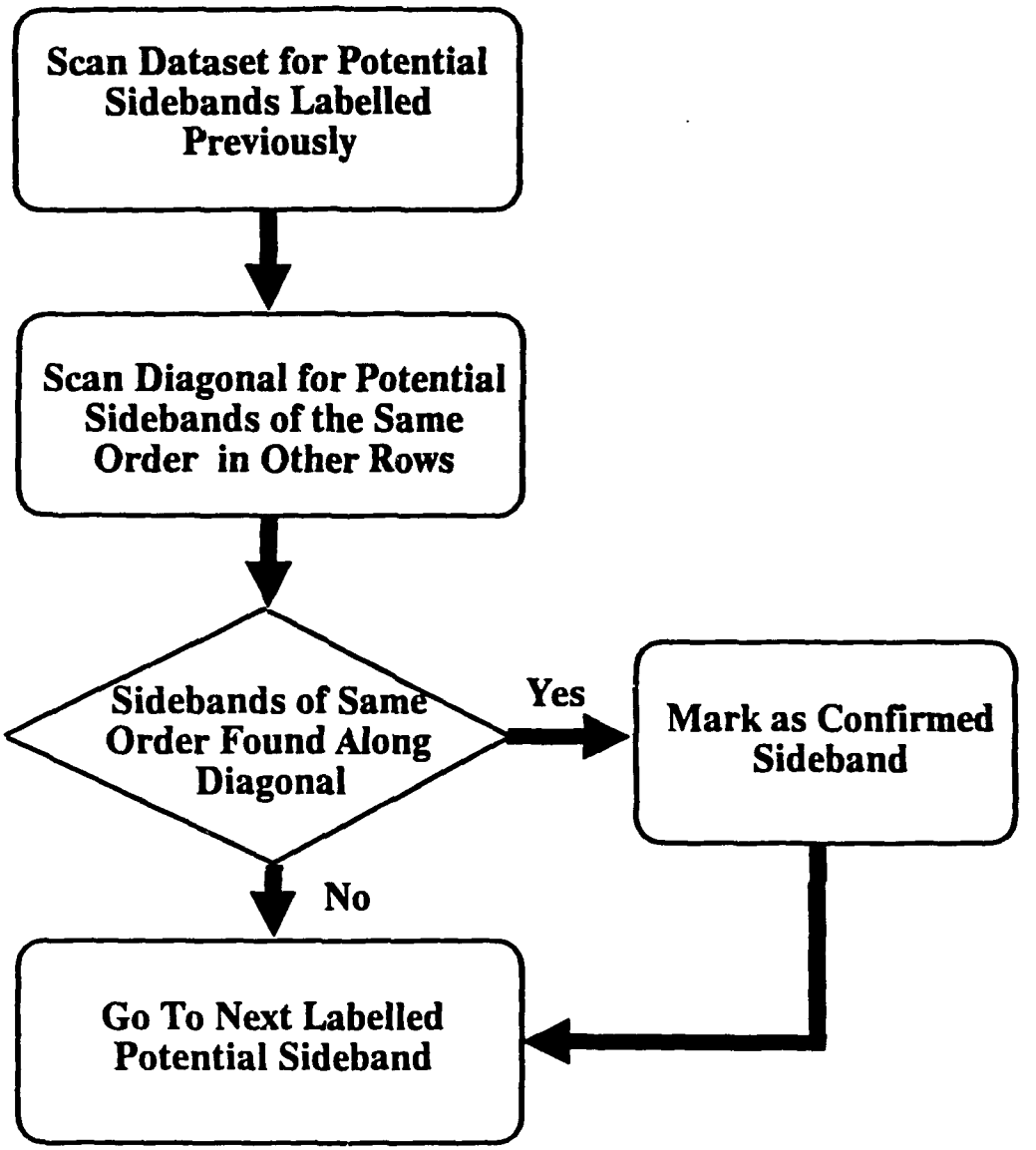
Scan Dataset for Potential Sidebands Labelled Previously
Scan Diagonal for Potential Sidebands of the Same Order in Other Rows
Sidebands of Same Order Found Along Diagonal
Yes
Mark as Confirmed Sideband
No
Go To Next Labelled Potential Sideband

RECONSTRUCTION

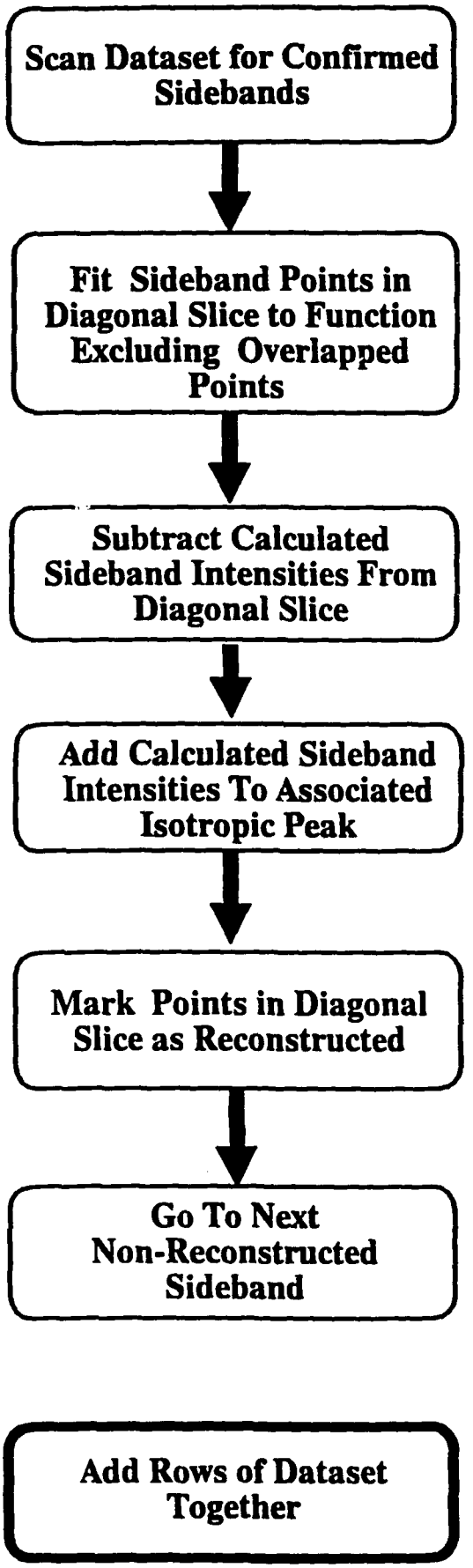

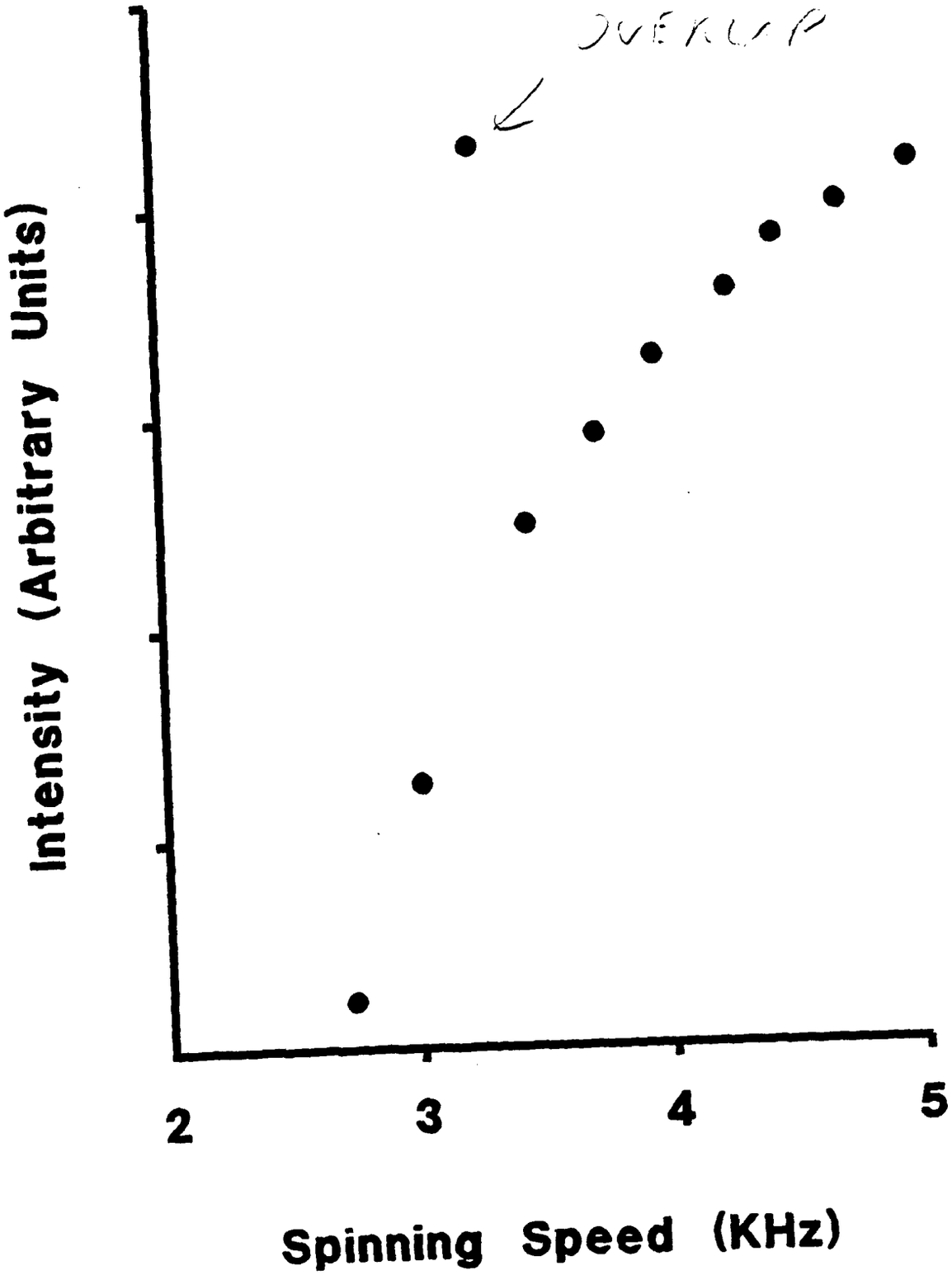
OVERLAP
Intensity (Arbitrary Units)
2
3
4
5
Spinning Speed (KHz)

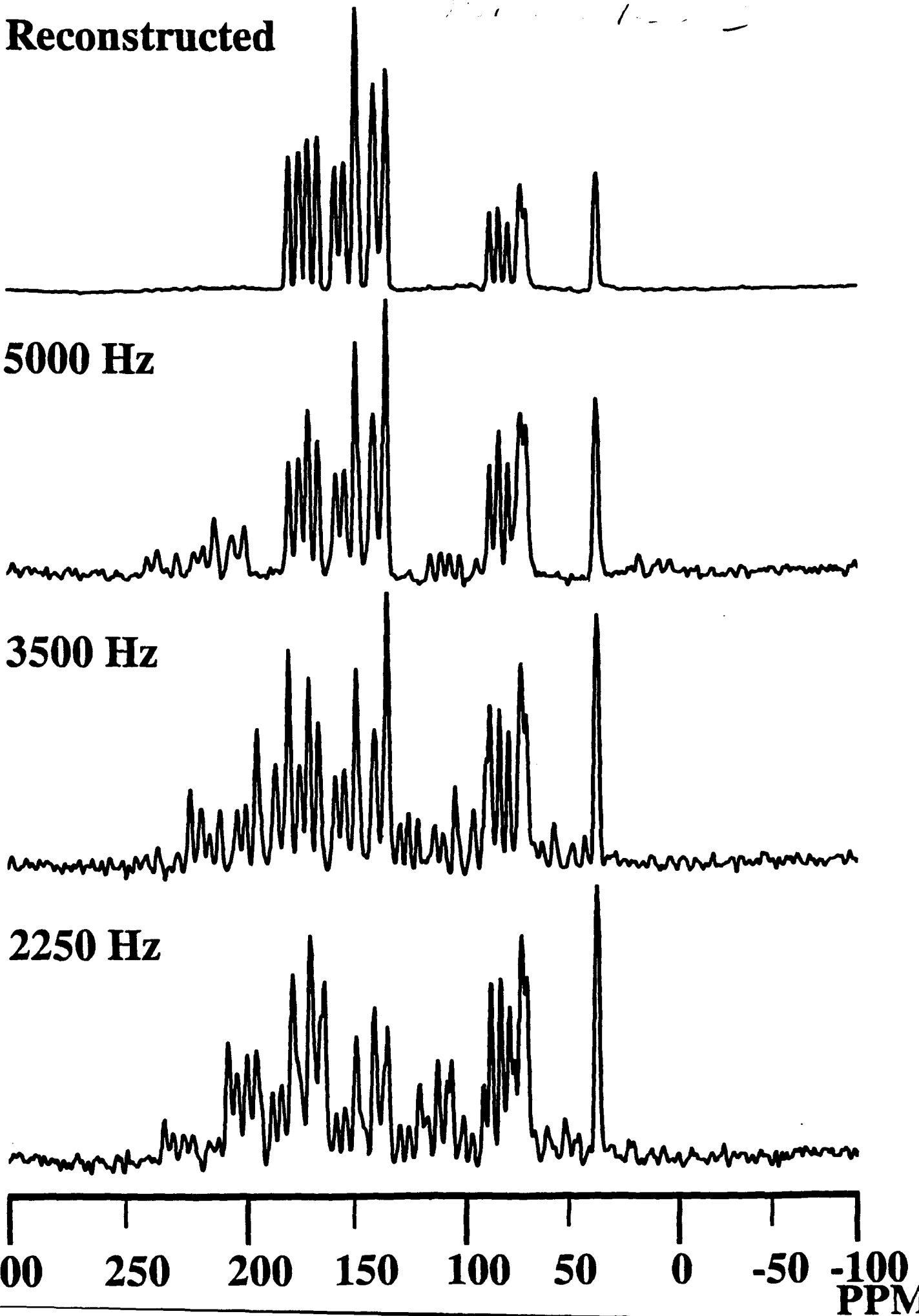
Reconstructed
5000 Hz
3500 Hz
2250 Hz
300
250
200
150
100
50
0
-50
-100
PPM

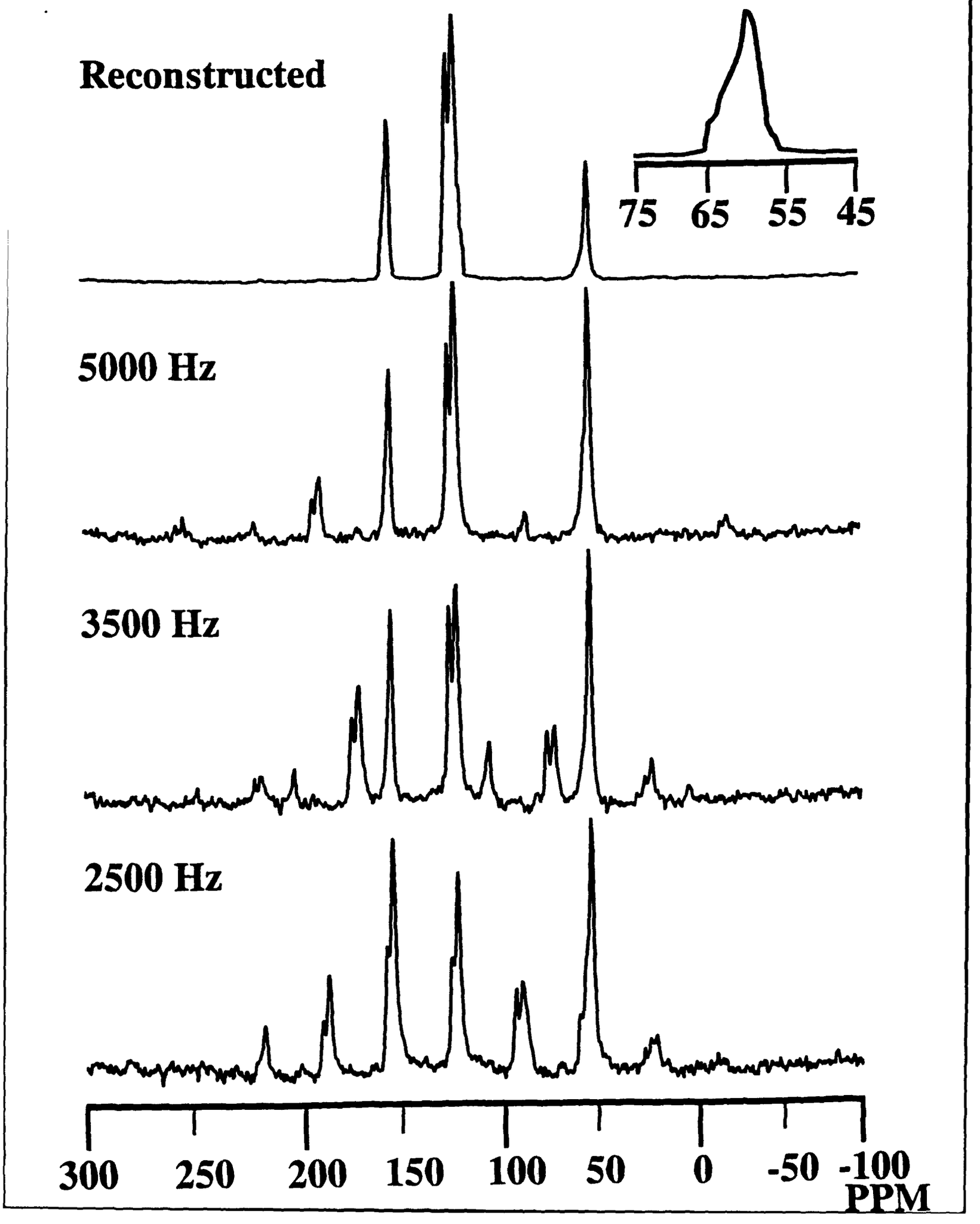
Reconstructed
75
65
55
45
5000 Hz
3500 Hz
2500 Hz
300
250
200
150
100
50
0
-50
-100
PPM

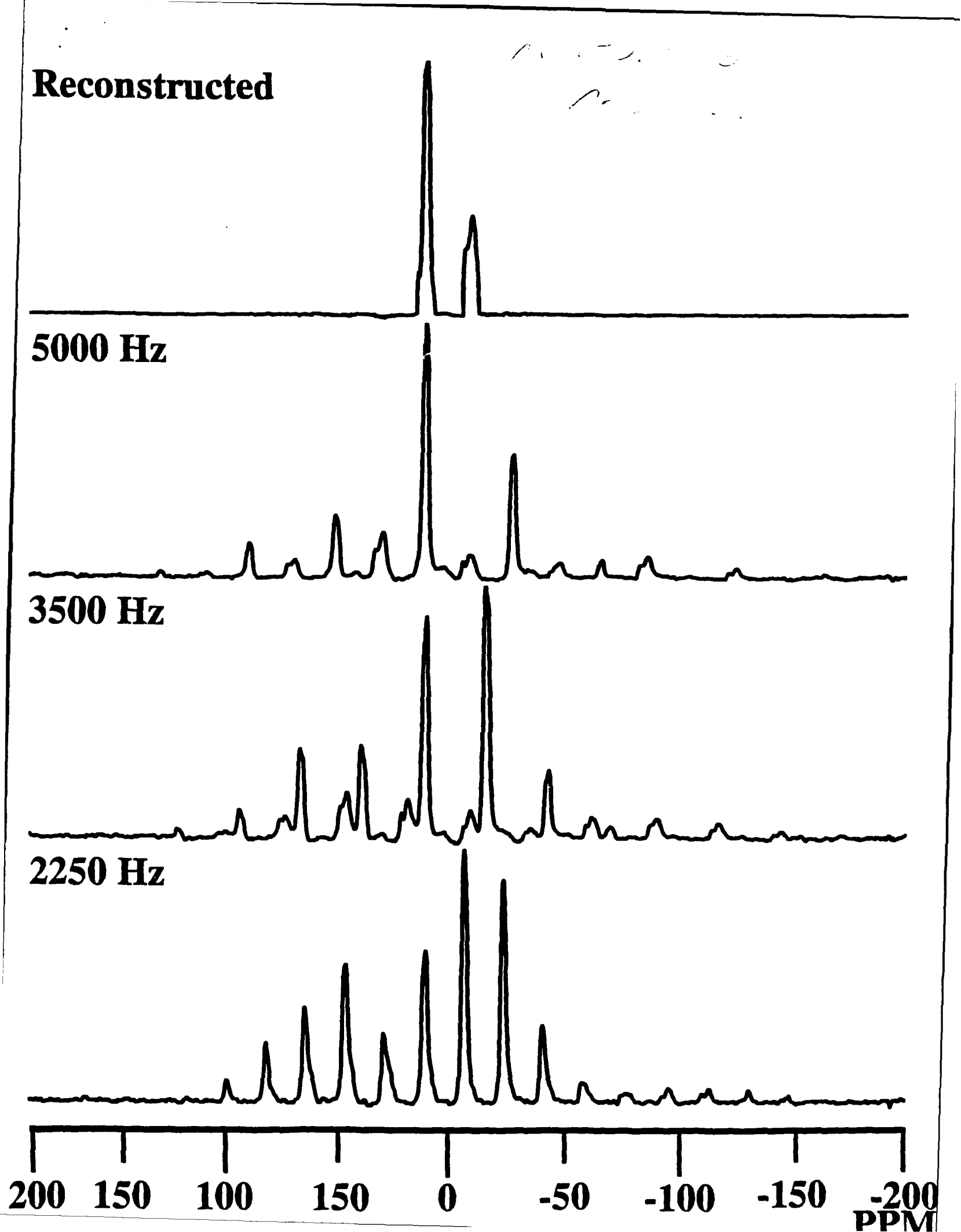
Reconstructed
5000 Hz
3500 Hz
2250 Hz
200 150 100 150 0 -50 -100 -150 -200
PPM

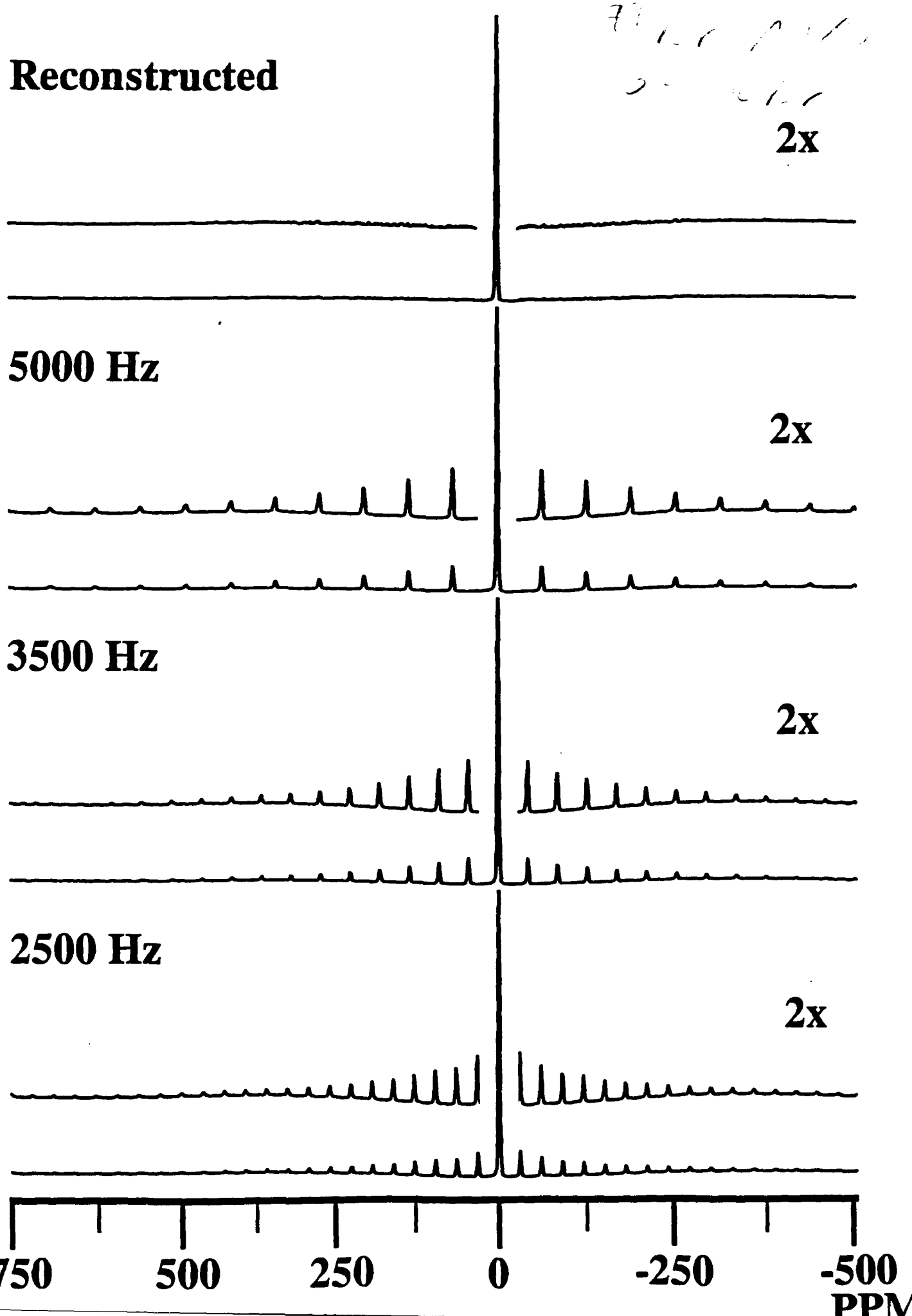
Reconstructed
2x
5000 Hz
2x
3500 Hz
2x
2500 Hz
2x
750
500
250
0
-250
-500
PPM

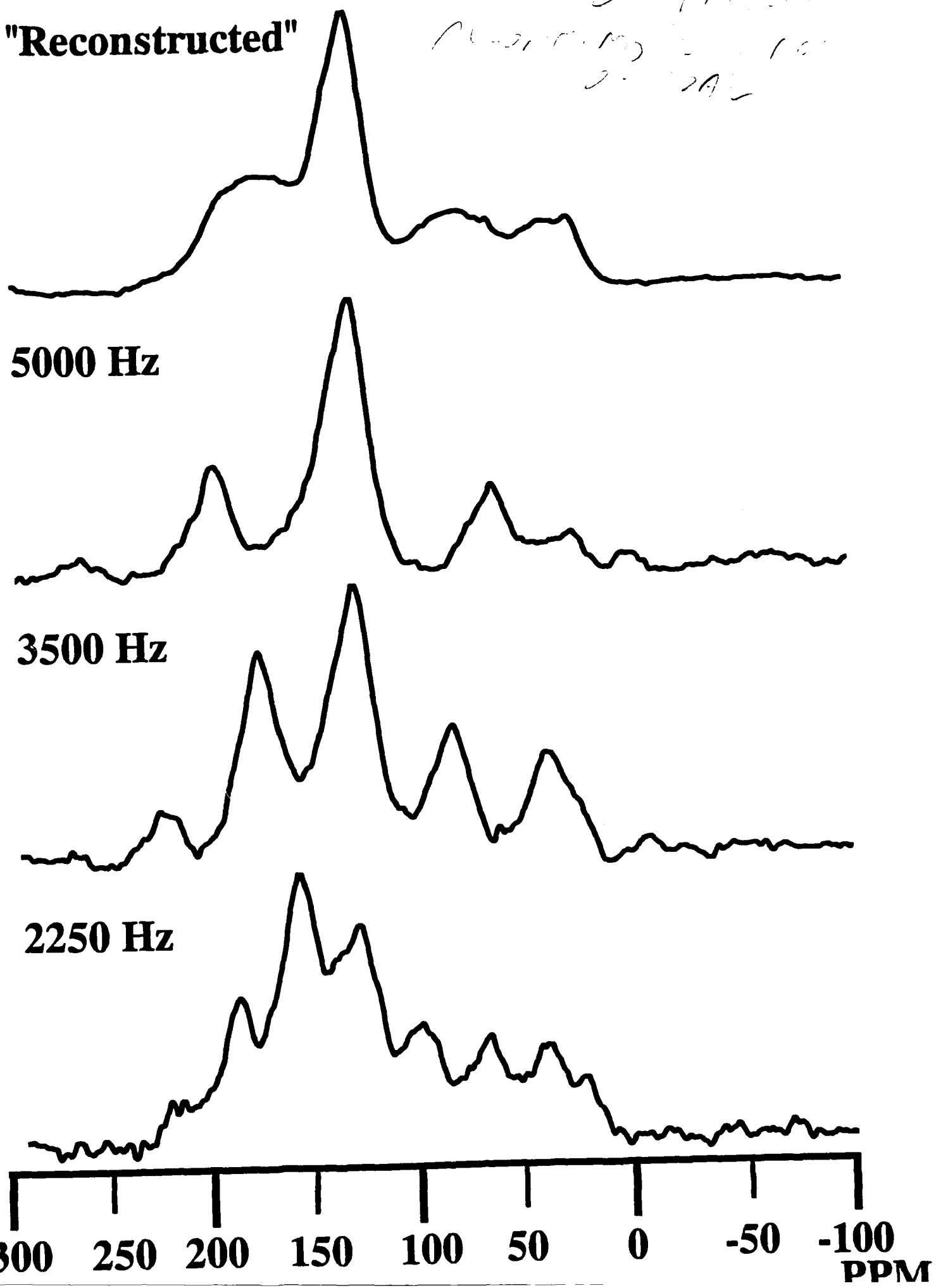
"Reconstructed"
5000 Hz
3500 Hz
2250 Hz
300
250
200
150
100
50
0
-50
-100
PPM